

Article

Experimental Determination of the Performances during the Cold Start-Up of an Air Compressor Unit for Electric and Electrified Heavy-Duty Vehicles

Gianluca Valenti ^{1,*}, Stefano Murgia ², Ida Costanzo ², Matteo Scarnera ¹ and Francesco Battistella ¹

¹ Department of Energy, Politecnico di Milano, Via Lambruschini 4/A, 20156 Milano, Italy; matteo.scarnera@mail.polimi.it (M.S.); francesco.battistella@polimi.it (F.B.)

² Ing. Enea Mattei S.p.A, Strada Padana Superiore 307, Vimodrone, 20055 Milano, Italy; stefano.murgia@matteigroup.com (S.M.); ida.costanzo@matteigroup.com (I.C.)

* Correspondence: gianluca.valenti@polimi.it

Abstract: Compressed air is crucial on an electric or electrified heavy-duty vehicle. The objective of this work was to experimentally determine the performance parameters of the first prototype of an electric-driven sliding-vane air compressor, specifically designed for electric and electrified heavy-duty vehicles, during the transient conditions of cold start-ups. The transient was analyzed for different thermostatic temperatures: 0 °C, −10 °C, −20 °C, and −30 °C. The air compressor unit was placed in a climatic chamber and connected to the electric grid, the water-cooling loop, and the compressed air measuring and controlling rig. The required start-up time was greater the lower the thermostatic temperature, ranging from 30 min at 0 °C to 221 min at −30 °C and depending largely on the volume of the lubricant oil filled initially. The volume flow rate of the compressed air was lower than nominal at the beginning, but it showed a step increase well beyond nominal when the oil reached 50 °C and then decreased gently towards nominal, while the input power kept steady at nominal after a short initial peak. These facts must be considered when estimating the time and the energy required by the air compressor unit to fill up the compressed air tanks of the vehicles.

Keywords: transport sector; positive-displacement compressor; sliding-vane compressor; climatic chamber; transient behavior



Citation: Valenti, G.; Murgia, S.; Costanzo, I.; Scarnera, M.; Battistella, F. Experimental Determination of the Performances during the Cold Start-Up of an Air Compressor Unit for Electric and Electrified Heavy-Duty Vehicles. *Energies* **2021**, *14*, 3664. <https://doi.org/10.3390/en14123664>

Academic Editor: João Pedro Trovao

Received: 12 May 2021
Accepted: 18 June 2021
Published: 19 June 2021

Publisher's Note: MDPI stays neutral with regard to jurisdictional claims in published maps and institutional affiliations.



Copyright: © 2021 by the authors. Licensee MDPI, Basel, Switzerland. This article is an open access article distributed under the terms and conditions of the Creative Commons Attribution (CC BY) license (<https://creativecommons.org/licenses/by/4.0/>).

1. Introduction

Today, the transport sector consumes 49% of the planet oil production and generates 27% of the overall anthropogenic carbon dioxide emission, causing a critical impact on the energy resources as well as on the local and the global environments [1,2]. In this sector, freight transport and non-urban public transport, which employ heavy-duty vehicles, are expected to become even more significant worldwide in the short-term future [3]. Carbon dioxide emissions of such vehicles can be as high as 25% of road transport emissions as a whole [4]. In response to the potentially larger and larger energy and environmental issues, electric vehicles have been proposed as an urgent countermeasure, with a global fleet expected to rise from 8.5 million in 2020 to 116 million vehicles in 2030, and a 28% share on the new sales [5]. In addition to the diffusion of electric vehicles, vehicle electrification, which is the electrification of the sole auxiliaries but not of the powertrain, has also been suggested as an effective countermeasure to reduce energy consumptions [6]. Rupp et al. highlight the potential reduction in emissions related to electrification in heavy-duty vehicles [7]. Unsurprisingly, the global outlook on electric vehicles by the International Energy Agency states that the electrification of heavy-duty vehicles represents an opportunity to be seized by manufacturers in the next decade [8].

Onboard an electric vehicle, the auxiliaries account for a fraction of 5–15% of the battery consumption when the vehicle itself moves at a speed of 60 km/h [9]. In heavy-duty vehicles, the auxiliaries with the highest energy consumption are the power steering

unit and the air compressor unit. Pettersson and Johansson showed that the consumption of auxiliaries in trucks powered by an internal combustion engine is 4–7% of the total energy consumption. They underlined that the impact of auxiliaries and their control strategy on the overall efficiency of the vehicle is mentioned in literature, although their accurate modeling is a quite unexplored area [10]. The effect of downsizing and of a better control strategy due to auxiliary electrification was simulated by Pretsch and Winter, who investigated the power steering unit and the air compressor unit predicting fuel savings of 3% [11]. The importance of the electrification of the main auxiliaries was also underlined by Kulikov et al., who showed that the power consumption by the air compressor unit and the power steering unit accounts for 55% of the overall auxiliary load in urban driving [6].

Compressed air on electric or electrified heavy-duty vehicles is mainly employed to actuate the brakes and the springs. The core of the air compressor unit is the air compressor that, on one side, consumes electricity, and on the other, requires a coolant. The control strategy of air compressor units was investigated by Tretsiak et al., who highlighted the benefit of a closed-loop control system and numerically proved a 24.3% reduction of battery energy consumption by the compressor itself [12]. The cooling system of the air compressor usually takes advantage of the engine coolant. In electric heavy-duty vehicles, the cooling system is expected to exploit the coolant after the electric motor and the power electronics, resulting in an inlet temperature of 80 °C. In fact, the loop of the cooling system taking care of the electric motor and the power electronics has a temperature of 75–80 °C [13]. In electrified heavy-duty vehicles, the cooling system exploits the coolant of the internal combustion engine, resulting in an inlet temperature higher than 80 °C.

The benchmark for the evaluation of air compressor packages for stationary application is the standard ISO 1217, which provides specifications for the acceptance tests, with a dedicated procedure for electric-driven positive-displacement compressors in its Annex C. The standard defines as reference conditions an ambient air at 20 °C, 100 kPa, and 0% relative humidity. Moreover, it includes as performance parameters the volume flow rate, the input power, and the specific energy requirement. Apart from this standard, there seems to be no other national or international reference documentation specifically for the transportation sector; therefore, electric and electrified vehicle manufacturers have their own testing protocols for air compressor units under diverse operating conditions.

The objective of the present work was to experimentally determine the performance parameters of the first prototype of an electric-driven sliding-vane air compressor, specifically designed for electric and electrified heavy-duty vehicles, during the transient conditions of cold start-ups. Among the performance parameters, the lubricant oil temperature as detected in the lubricant tank was analyzed to assess the time required for the whole transient to be completed. Cold start-ups are considered particularly challenging because of the low temperature and, hence, the high viscosity of the lubricant oil, which might negatively affect the functionality and the performances of the air compressor unit.

The methodology was based on an experimental campaign in which the air compressor unit was placed inside a climatic chamber to emulate cold conditions. The cold start-up transient was analyzed for different thermostatic temperatures: 0 °C, −10 °C, −20 °C, and −30 °C. During the tests the air compressor discharge pressure was controlled at 1.0 MPa, which is the upper bound of air pressure levels in heavy-duty vehicles [14]. The temperature in the lubricant tank, the air volume flow rate, the input power, and volume-to-power ratio were recorded for all tests and reported here normalized with respect to the nominal performance parameters at 20 °C. The volume-to-power ratio is numerically the reciprocal of the specific energy requirement defined in ISO 1217; this ratio was preferred here because it is more immediate for the design of the electric circuit of an electric or electrified vehicle. Lastly, each thermostatic temperature was replicated on at least two different days for repeatability.

To our knowledge, the literature has not specifically assessed the experimental determination of the performances of an electric-driven air compressor during cold start-up transients in a climatic chamber. In an analogue investigation, van Gompel and Koornneef

described an impressive climatic-altitude chamber for testing whole heavy-duty vehicles and powertrains, but not air compressors [15]. In another, Li et al. presented an accurate method for measuring the performances of reciprocating air compressors, but not under severe climatic conditions [16]. Conceptually, the present work combines both approaches. Continuing on a preceding activity [17], this work provides a full set of information for developing numerical models and control logics of air compressor units for electric and electrified heavy-duty vehicles and, in general, for designing preliminarily these units.

The following sections describe the experimental setup, the experimental results and their discussion, the general recommendations, and ultimately the work's conclusions.

2. Experimental Setup

The experimental setup was realized and conducted at the Laboratory of Energy Conversion and Storage of Politecnico di Milano. This section describes the air compressor unit under investigation; the test rig and the instruments employed in the campaign; and, finally, the testing procedure executed for all the tests at each thermostatic temperature.

2.1. Air Compressor Unit

The air compressor unit, designed specifically for electric and electrified heavy-duty vehicles and tested inside the climatic chamber, is illustrated by Figure 1. It comprises an intake air filter, an air compressor connected to an electric motor, an air/oil separator, which acts also as lubricant tank, a coalescence filter, an oil filter, and a cooling system based on an oil-water heat exchanger. The air compressor is a sliding-vane compressor that incorporates a lubricant oil injection system with an oil spraying nozzle to ensure a very good lubrication of the compressor and a very effective cooling of the air during compression to minimize the power consumption [18]. The air/oil separator unit exploits an inertial principle to recover over 99% of the oil mixed in the compressed air stream. The remaining oil is recovered in the coalescence filter located after the separator. The flow of the lubricant oil to the heat exchanger is governed by a thermostatic valve, which opens when the lubricant oil temperature approaches 70 °C. Moreover, the air compressor unit features a patented anti-condensation valve and control logic that recircles part of the compressed and hot air to the compressor intake to heat it by staying open while the lubricant temperature is lower than 50 °C. Lastly, the unit features a patented oil recovery valve and control logic that transfers the oil collected by the coalescence filter to the air compressor intake by opening discontinuously [19–22]. The valve stays open for 1% of the time between each opening. Based on the results from this campaign, the time parameters of the valve opening will be improved to minimize the recycled air. Lastly, the electric motor mounted on this prototype is a 2.2-kW and 1760-rpm asynchronous one for industrial stationary applications because it is connected to the national electric grid, while that for an electric or electrified vehicle will likely be of a different kind. Permanent magnet motors seem to be more commonly applied on electric and electrified vehicles.

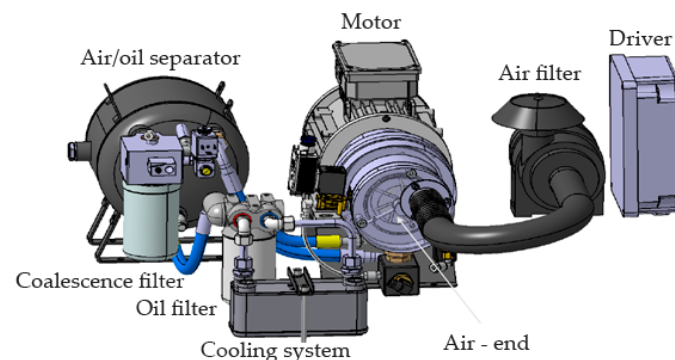


Figure 1. Schematic of the first prototype of the air compressor unit designed specifically for electric and electrified heavy-duty vehicles and tested inside a climatic chamber in the present work.

2.2. Experimental Rig

The experimental rig, composing of the air compressor unit placed in the climatic chamber and the measuring and controlling rig located outside of the chamber, is pictured in Figure 2. The air compressor unit was connected to the electric grid and to a cooling water loop to replicate the boundary conditions of the installation on a heavy-duty vehicle (Figure 2a). In this campaign investigating the cold start-ups, though, cooling water was never provided to the compressor because the tests ended when the lubricant tank reached 80 °C. The air compressor unit was equipped with three temperature sensors and one pressure transducer. The sensors were located in the lubricant tank and taken as reference during the cold start-up, in the oil line to the heat exchanger, and in the oil line from it; the transducer was also located at the lubricant tank. The measuring and controlling rig, connected to the air compressor discharge, was equipped with a redundant temperature sensor at the inlet of the rig, a manual regulation valve, a pressure transducer and regulator, two condensate separators for the protection of the downstream instruments, a thermal mass flow meter, and a silencer (Figure 2b). The pressure transducer and regulator were utilized to control the air discharge pressure.

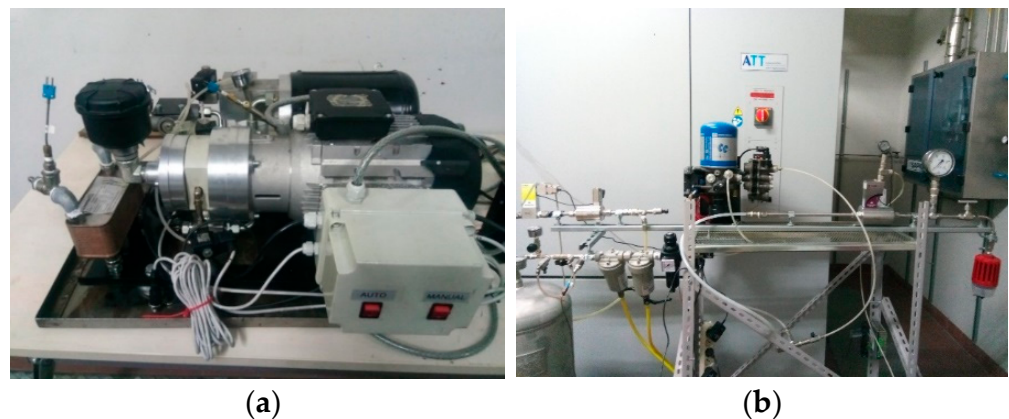


Figure 2. The experimental rig: (a) the air compressor unit to be placed inside the climatic chamber; (b) the measuring and controlling rig located outside of the climatic chamber.

The climatic chamber was the model Discovery DY 1200, manufactured by Angelantoni (Italy), which is capable of producing temperatures between -40 °C and $+180$ °C and relative humidity between 10% and 98%, either in steady state conditions or following user-defined cycles. Furthermore, the instruments for mass flow rate, pressure, and temperature were connected to a cDAQ controller and acquired by a specifically developed code in LabVIEW, both by National Instruments (U.S.A.). All these data were gathered synchronously. The electric power meter was connected to that computer and acquired via the software by FLUKE (Germany). The process flow diagram of the experimental rig is visualized in Figure 3, while the instrument characteristics are listed in Table 1.

Table 1. Instruments employed in the tests. Rd stands for read value, while Fs stands for full scale; the flow rate refers to normal conditions of 0 °C and 101.325 kPa (absolute).

Parameter	Unit	Instrument	Accuracy
(Mass) flow rate (M1)	m ³ /h	Bronkhorst F-113AI	$\pm 0.5\%Rd \pm 0.1\%Fs$
Pressure (P2)	Pa	Bronkhorst EL-PRESS P-502C	$\pm 0.5\%Fs$
Current	A	FLUKE 1748	$\pm 1\%Rd \pm 0.02\%Fs$
Voltage	V	FLUKE 1748	$\pm 0.1\%Rd$
Temperature (T1 to T4)	°C	T-type thermocouple	0.5 °C

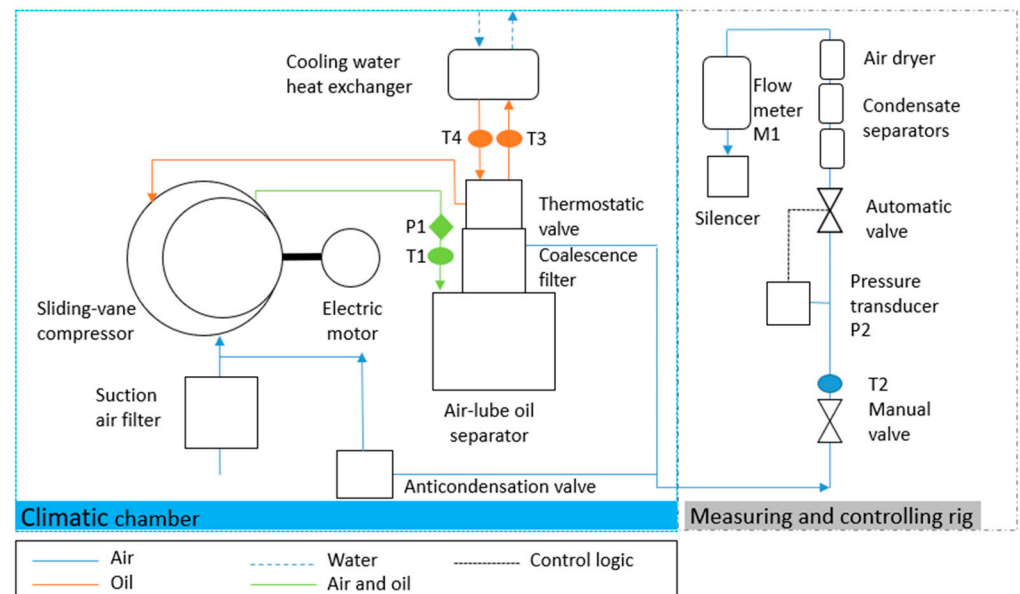


Figure 3. Process flow diagram of the experimental rig, showing the air compressor unit placed inside the climatic chamber as well as the measuring and controlling rig.

2.3. Experimental Procedure

The performance parameters considered in the present work are:

- the temperature in the lubricant tank,
- the start-up time, which is the time the temperature in the lubricant tank reached $80\text{ }^{\circ}\text{C}$,
- the volume flow rate at the air compressor discharge,
- the air compressor input power, and
- the volume-to-power ratio, which is the ratio of the flow rate and the input power.

The thermostatic temperatures were $0\text{ }^{\circ}\text{C}$, $-10\text{ }^{\circ}\text{C}$, $-20\text{ }^{\circ}\text{C}$, and $-30\text{ }^{\circ}\text{C}$. At least two independent tests were performed for each thermostatic temperature to verify the repeatability between the tests. Moreover, the order of the executed tests was random in order to exclude any systematic error. The timespan required for each test was variable and was based on the lubricant oil temperature in the lubricant tank, concluding the test when it reached $80\text{ }^{\circ}\text{C}$. During the test, the coolant was not flowing into the cooling system of the air compressor unit to allow for a start-up as fast as possible.

Every test started with setting the climatic chamber at the desired thermostatic temperature and waiting until the temperature was stable both in the climatic chamber itself and the air compressor unit. Then, the air compressor unit was switched on, while the pressure at its discharge was controlled at 1.0 MPa . It was turned off when the temperature of the lubricant tank reached $80\text{ }^{\circ}\text{C}$. During all tests considered, the thermostatic temperature inside the climatic chamber remained close by a few degrees to the desired value.

3. Experimental Results and Discussion

This section presents the results in four charts: temperature in the lubricant tank, normalized volume flow rate at the air compressor discharge, normalized input power to the compressor, and normalized volume-to-power ratio for all the thermostatic temperatures. Normalization was computed against the nominal performance parameters at $20\text{ }^{\circ}\text{C}$. Each chart shows the results for a given temperature averaged over the tests executed for that temperature. The tests at each temperature were repeated twice, except for at $-10\text{ }^{\circ}\text{C}$ which was repeated three times, while at $-30\text{ }^{\circ}\text{C}$ was repeated twice, but one test was discarded as explained next. For completeness, the results of each test are provided in Appendix A. These results showed a high repeatability and accurate control of

the thermostatic temperature, except for one test at $-30\text{ }^{\circ}\text{C}$; hence, this specific test was discarded from the analysis and only the other one was retained. Ultimately, the main performances were tabulated.

Figure 4 illustrates the temperature during the cold start-up transient for the diverse thermostatic temperatures. All curves are characterized by an initial plateau at the thermostatic temperature followed by a steep increase. Then, the temperature slope decreases continuously towards zero at approximately $70\text{ }^{\circ}\text{C}$, at which oscillations occur. Ultimately, after the oscillations, a milder increase starts. The initial plateau is larger the lower the thermostatic temperature, and this is likely related to the time required for the oil to circulate through the compressor. In fact, the lower the temperature the higher the viscosity and, hence, the lower the flow rate. Moreover, the steep increase is actually steeper the higher the thermostatic temperature, and this is likely related to the lower heat transfer between the air compressor unit and the thermostatic temperature. The oscillations at $70\text{ }^{\circ}\text{C}$ are instead related to the relatively slow opening of the thermostatic valve that let the oil flow into the heat exchanger that was still cold at that moment. The oscillations last longer the lower the thermostatic temperature, likely, again, due to the higher heat transfer from the air compressor unit to the external air. The same occurs for the milder increase following the oscillations. The transient was considered concluded at $80\text{ }^{\circ}\text{C}$, which is the reference temperature for the coolant. The start-up time required for the whole transient was larger the lower the thermostatic temperature. It ranged from 30 min at $0\text{ }^{\circ}\text{C}$ to 221 min at $-30\text{ }^{\circ}\text{C}$. In the previous work by Valenti et al. [17], the start-up times were lower, for example 69 min at $-30\text{ }^{\circ}\text{C}$, because in the present experimentation, a much higher oil quantity was initially filled into the lubricant tank. This decision proves that the oil quantity has a direct influence on the cold startup-up transient.

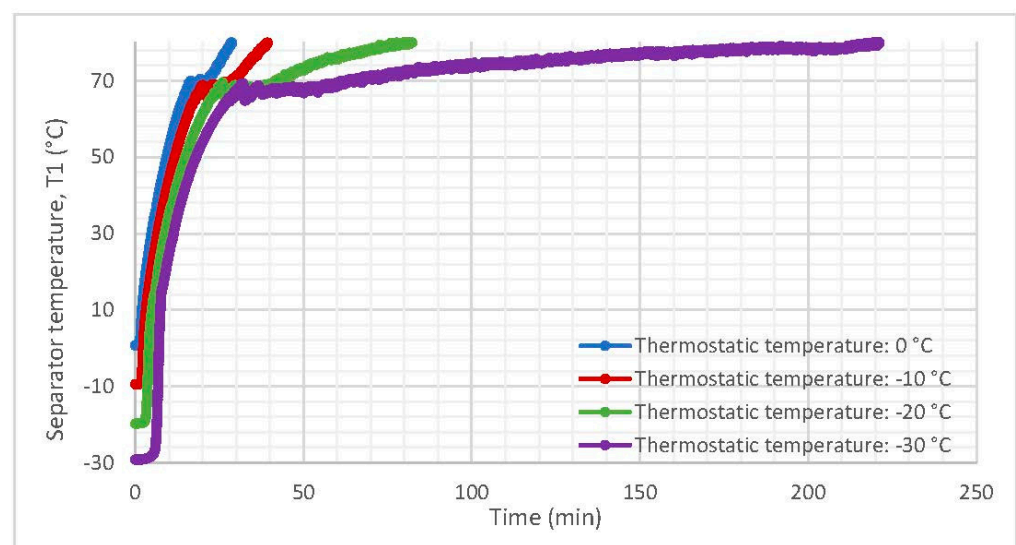


Figure 4. Temperature in the air/oil separator, acting also as lubricant tank, averaged over the two tests executed for the diverse thermostatic temperatures.

Figure 5 represents the normalized volume flow rate during the cold start-up transient. The data were normalized with respect to the nominal volume flow rate at $20\text{ }^{\circ}\text{C}$. All curves are characterized by an initial plateau followed by a step increase and, lastly, by a gentle decrease; moreover, all curves are characterized by sudden and short drops of flow rate due to oil recovery valve opening. The initial plateau is longer the lower the thermostatic temperature, however the flow rate after the step increase is higher the lower the thermostatic temperature. The initial plateau is due to the anti-condensation valve that remained open until the lubricant oil reached $50\text{ }^{\circ}\text{C}$ in order to recirculate part of the compressed and hot air to the compressor intake. Therefore, the available air at the discharge of the compressor increased immediately as the valve closed. Furthermore, the

cause of the periodical points with much lower flow was the oil recovery valve, which opened discontinuously in order to empty the coalescence filter.

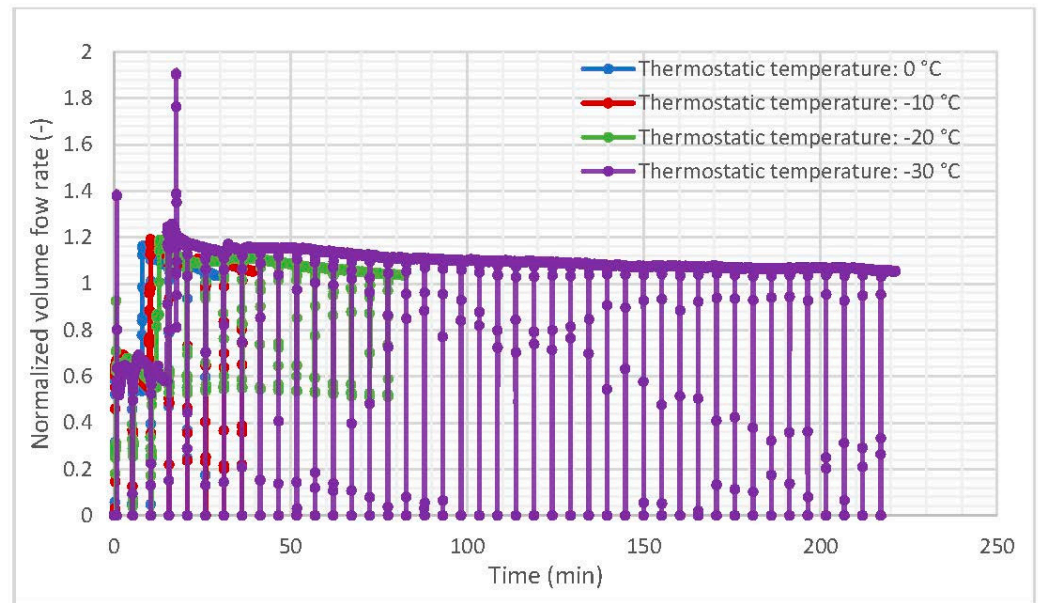


Figure 5. Normalized volume flow rate averaged over the two tests executed for the diverse thermostatic temperatures.

Figure 6 depicts the normalized input power. The data were normalized with respect to the nominal input power. All curves are characterized by a peak immediately after the start-up followed by a gentle asymptotic decrease. The peak is due to the inrush current, which is typical of an asynchronous motor, employed here for direct connection to the national electric grid. In contrast, motors for electric and electrified heavy-duty vehicles do not suffer from the inrush current because they are switched on by an inverter, electrically connected directly with the battery pack of the vehicle. The consumed power was stable at all thermostatic temperatures after the peak. Such a power was also consumed when the anti-condensation system was reducing the available discharge air flow rate.

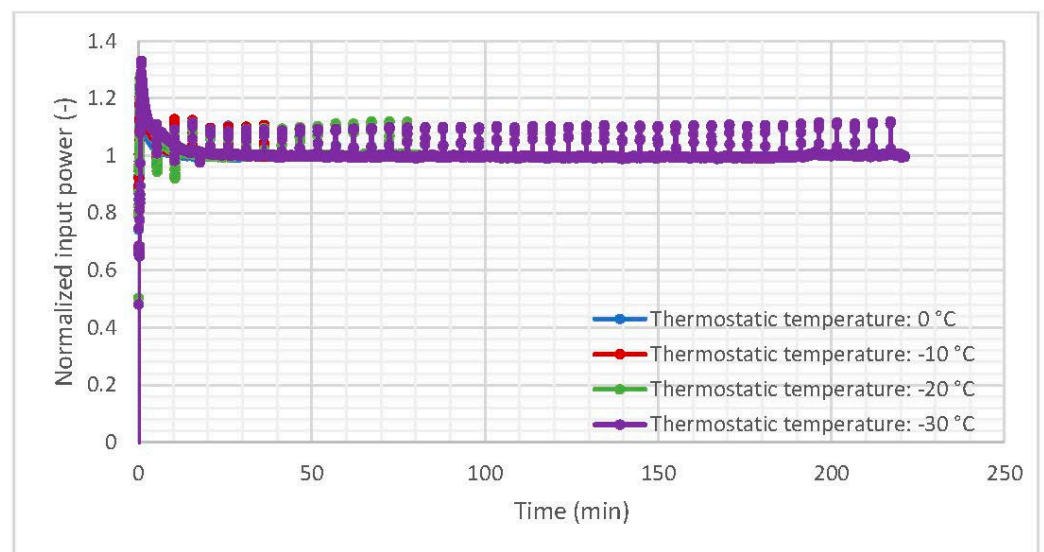


Figure 6. Normalized input power averaged over the two tests executed for the diverse thermostatic temperatures.

Figure 7 shows the normalized volume-to-power ratio, combining the information from Figures 5 and 6. The data were normalized with respect to the nominal ratio. All curves are similar to those of the volume flow rate, with the difference being that there is no initial plateau, but a steep increase due to the relatively constant volume flow rate, but the lowering input power from the initial peak. The volume-to-power ratio highlights the effect of the anti-condensation valve. The sudden increase on the volume-to-power ratio is related to the closing of the valve. The effect is an increase in the discharge air flow rate while consuming the same amount of power. The step increase of volume-to-power ratio happened later the lower the thermostatic temperature.

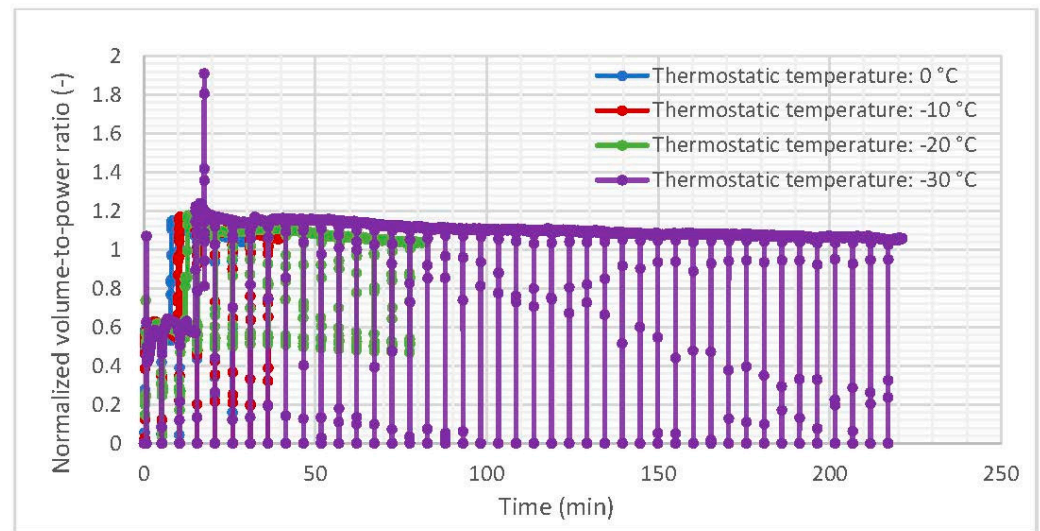


Figure 7. Normalized volume-to-power ratio averaged over the two tests executed for the diverse thermostatic temperatures.

Ultimately, Table 2 reports the main performance parameters of the present work. Among the parameters, the normalized volume flow rate and the normalized volume-to-power ratio are the mean values computed after the closing of the anti-condensation valve. The parameters show again that the start-up time was much longer the lower the thermostatic temperature; moreover, the volume flow rate as well as the volume-to-power ratio were slightly higher the lower that temperature.

Table 2. Main results averaged after the closing of the anti-condensation valve that recirculates compressed and hot air, when the oil temperature reaches 50 °C.

Temperature	Start-Up Time	Normalized Volume Flow Rate	Normalized Volume-to-Power Ratio
0 °C	28.8 min	107.0%	106.9%
−10 °C	39.3 min	108.0%	108.1%
−20 °C	82.3 min	108.2%	108.9%
−30 °C	221.2 min	115.1%	114.5%

4. General Recommendations

This section provides a set of general recommendations for the design of air compressor unit for electric and electrified heavy-duty vehicles as well as of the new prototype.

First of all, in cold climates at 0 °C or below, the cooling load of the air compressor unit is null for quite long periods, likely longer than engines, motors, and battery cooling loads. Moreover, the flow rate at the start-up is lower than nominal for periods that are longer the lower the temperature. This fact must be addressed when designing the air compressor unit for meeting the time required to fill up the compressed air tanks on a

heavy-duty vehicle. However, as soon as the anti-condensation valve closes, the flow rate immediately becomes high, and higher the lower the temperatures. In contrast, volume flow rates should be checked carefully in hot climates, which are not covered here. Initial input power peaks for the electric motors mounted on the vehicle should be verified.

The next prototype of the compressor will be characterized by an optimized timing of the anti-condensation valve opening, in order to minimize the recycled air, as well as an optimized volume of lubricant oil initially filled, in order to reduce the start-up time.

5. Conclusions

The present work reports the experimental investigation of the performances during a cold start-up transient of a prototype of a sliding-vane air compressor designed specifically for electric and electrified heavy-duty vehicles. The results are reported after experimental tests in a climatic chamber operating at the thermostatic temperatures of 0, −10, −20, and −30 °C. The parameters considered in the investigation were the temperature in the lubricant tank, the normalized volume flow rate of compressed air, the normalized input power, and the normalized volume-to-power ratio. The conclusions are as follows.

- The start-up time to heat the lubricant oil up to 80 °C varied significantly with the thermostatic temperature, ranging from 30 min at 0 °C to 221 min at −30 °C, depending largely on the volume of lubricant oil initially filled.
- The oil temperature followed very similar trends in all the tests, although the time lengths of each section of the curves were longer at lower temperatures.
- The volume flow rate of the compressed air was lower than nominal at the beginning, roughly 50–70% of the nominal value, but it showed a step increase when the oil reached 50 °C, and then it decreased gently towards nominal.
- The input power had a peak in the initial phase of operation, reaching almost 130% of the nominal value at the lower thermostatic temperature of −30 °C, but it reduced quite rapidly to the nominal input power for any thermostatic temperature.
- The volume-to-power ratio, which is related to air compressor efficiency, had a step increase when the volume flow rate increased. The increase happened later at lower temperatures, decreasing the overall efficiency during the cold start-up transient.
- Lastly, the air compressor functioned without issues in all the tests.
- In short, the cold start-up of an air compressor unit for electric and electrified heavy-duty vehicles can lead to lower cooling loads but also to lower volume flow rates and to initial peaks in input power, requiring an optimized timing of the valves.

Author Contributions: Conceptualization, S.M., I.C. and G.V.; methodology, G.V.; investigation, M.S. and F.B.; resources, S.M. and I.C.; data curation, F.B.; writing—original draft preparation, F.B.; writing—review and editing, G.V., S.M. and I.C.; visualization, G.V. and S.M.; supervision, G.V.; project administration, G.V.; funding acquisition, S.M. and G.V. All authors have read and agreed to the published version of the manuscript.

Funding: This work was funded partly by Regione Lombardia under the grant INNODRIVER 2017.

Institutional Review Board Statement: Not applicable.

Informed Consent Statement: Not applicable.

Conflicts of Interest: The authors declare no conflict of interest.

Appendix A

This Appendix reports the charts for the four performance parameters for each thermostatic temperature showing all the tests conducted.

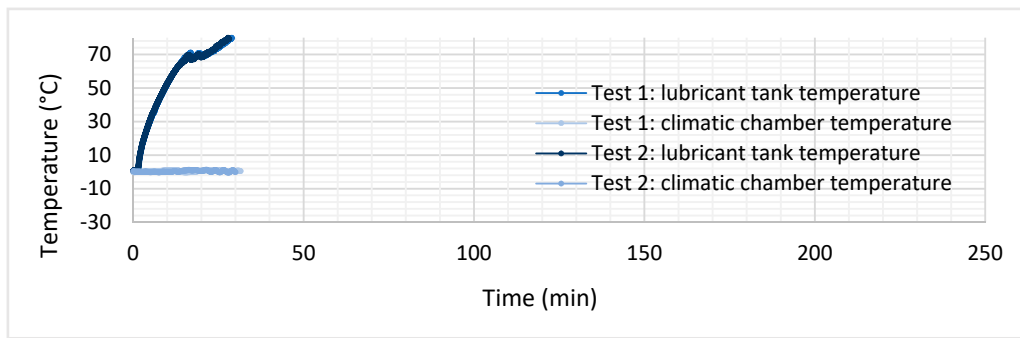


Figure A1. Lubricant tank and climatic chamber temperature trend at a thermostatic temperature of 0 °C during the two repetitions.

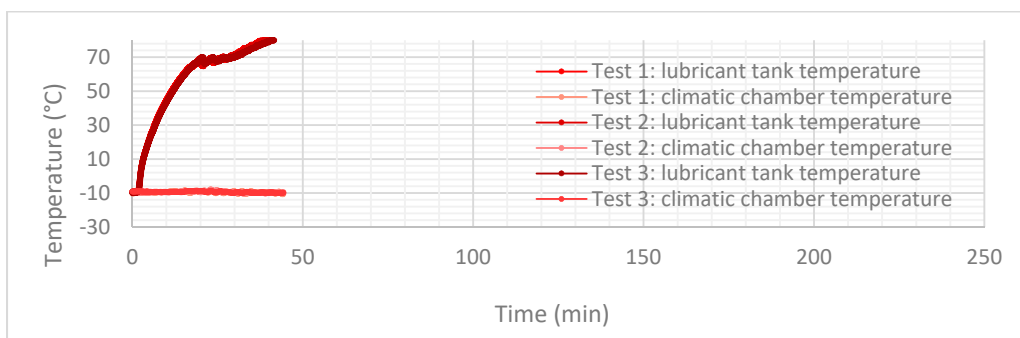


Figure A2. Lubricant tank and climatic chamber temperature trend at a thermostatic temperature of −10 °C during the three repetitions.



Figure A3. Lubricant tank and climatic chamber temperature trend at a thermostatic temperature of −20 °C during the two repetitions.

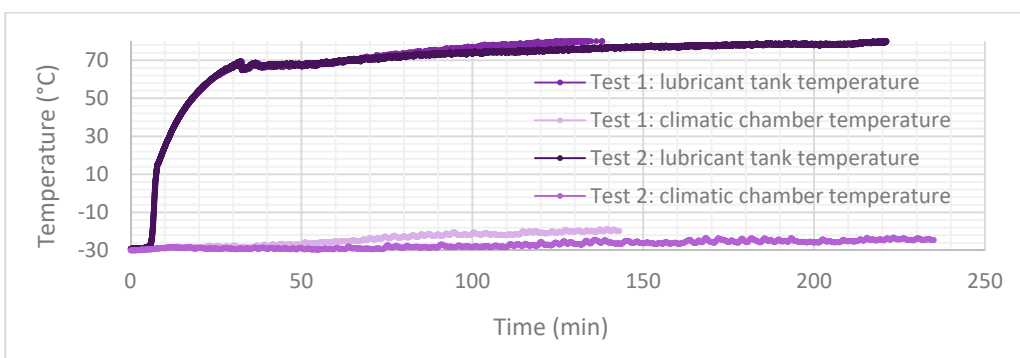


Figure A4. Lubricant tank and climatic chamber temperature trend at a thermostatic temperature of −30 °C during the two repetitions. During one of the repetitions, the thermostatic temperature was not steady.

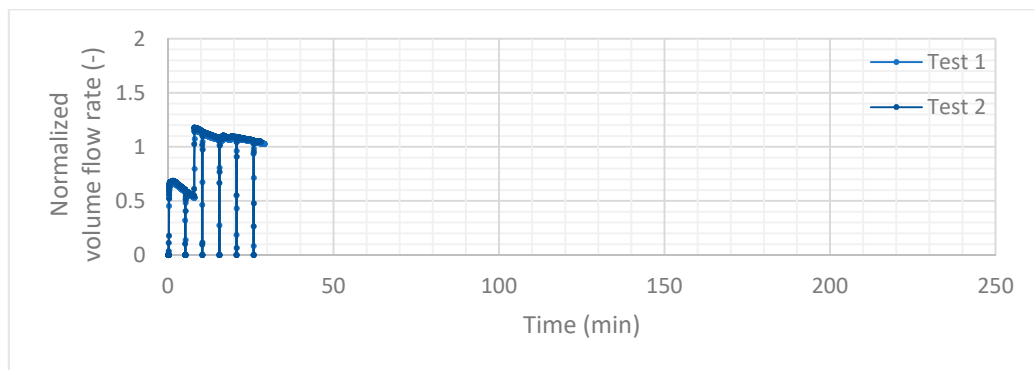


Figure A5. Normalized air volume flow rate trend at a thermostatic temperature of 0 °C during the two repetitions.

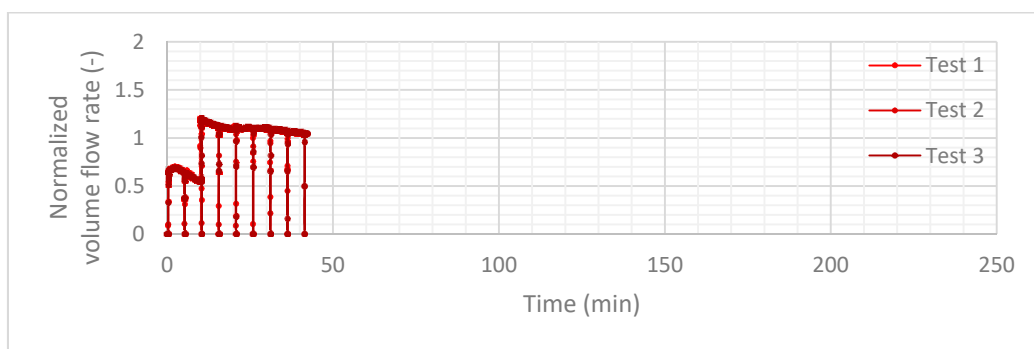


Figure A6. Normalized air volume flow rate trend at a thermostatic temperature of -10 °C during the three repetitions.

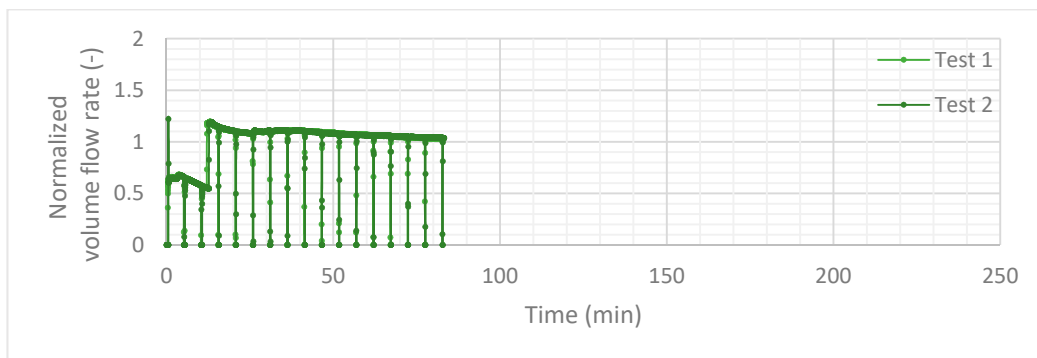


Figure A7. Normalized air volume flow rate trend at a thermostatic temperature of -20 °C during the two repetitions.

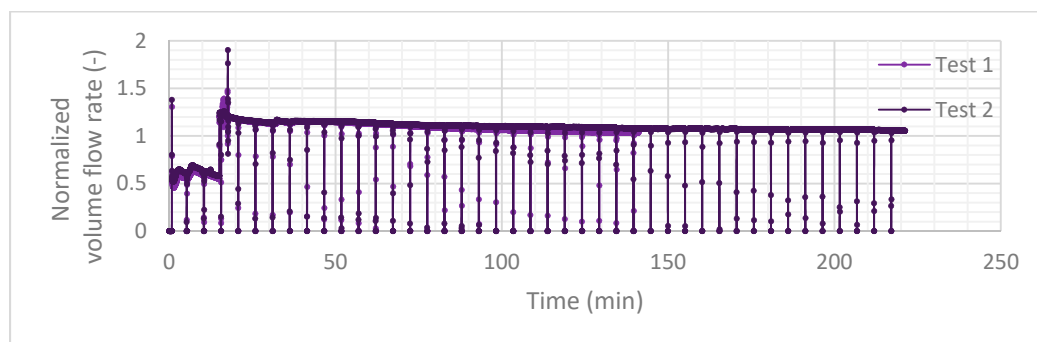


Figure A8. Normalized air volume flow rate trend at a thermostatic temperature of -30 °C during the two repetitions.

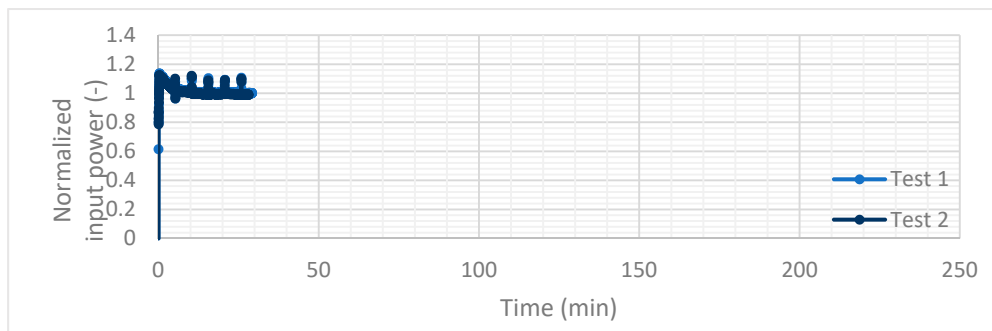


Figure A9. Normalized input power to the air compressor unit at the thermostatic temperature of 0 °C.

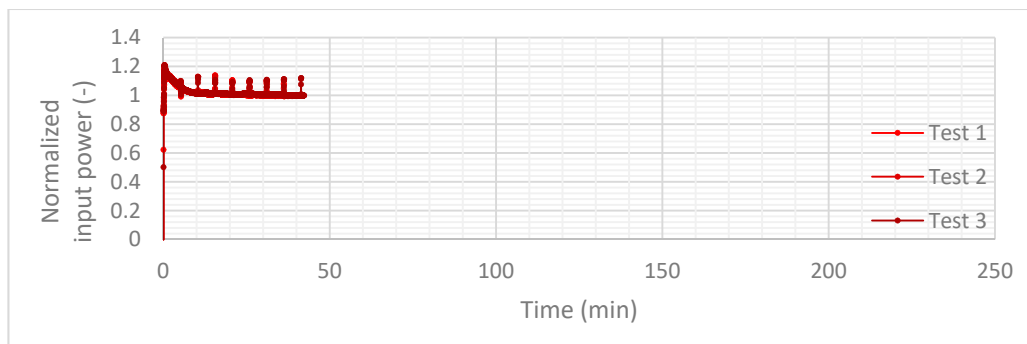


Figure A10. Normalized input power to the air compressor unit at the thermostatic temperature of -10 °C.

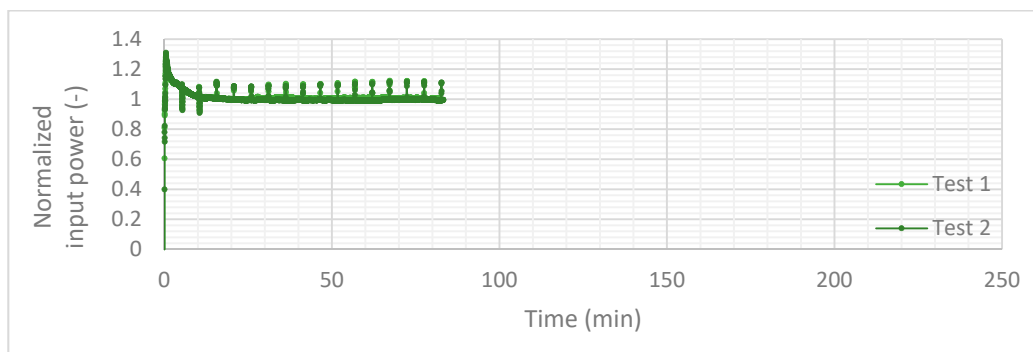


Figure A11. Normalized input power to the air compressor unit at the thermostatic temperature of -20 °C.

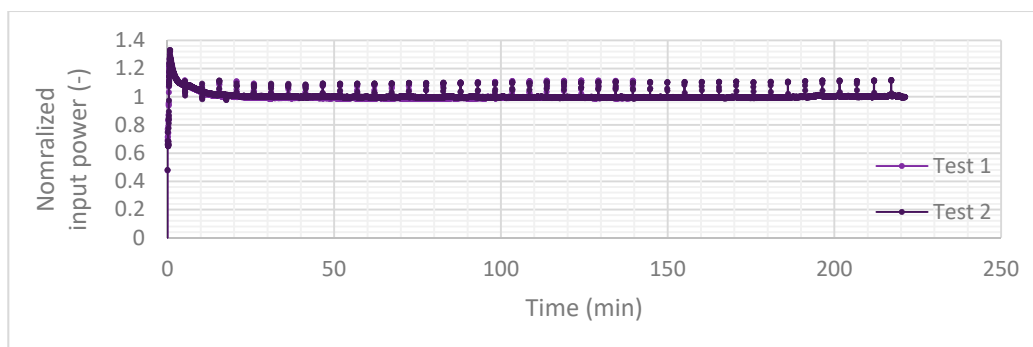


Figure A12. Normalized input power to the air compressor unit at the thermostatic temperature of -30 °C.

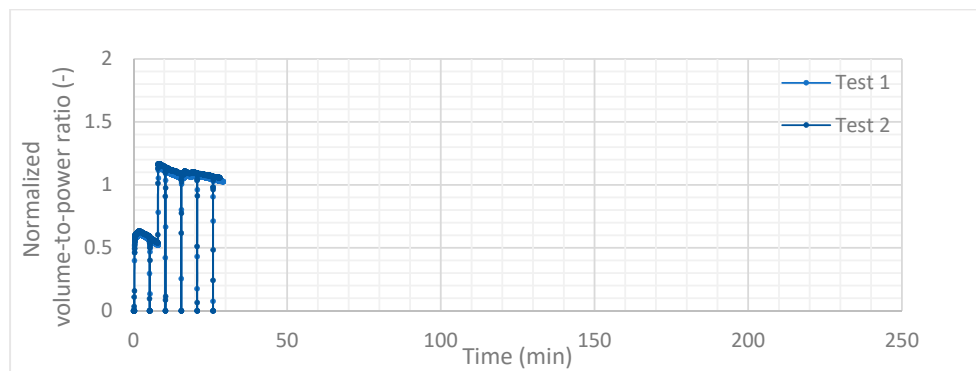


Figure A13. Normalized volume-to-power ratio at the thermostatic temperature of 0 °C.

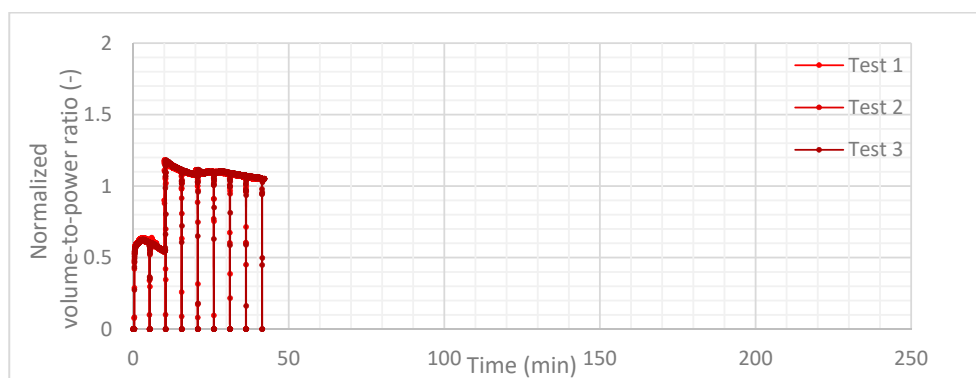


Figure A14. Normalized volume-to-power ratio at the thermostatic temperature of -10 °C.

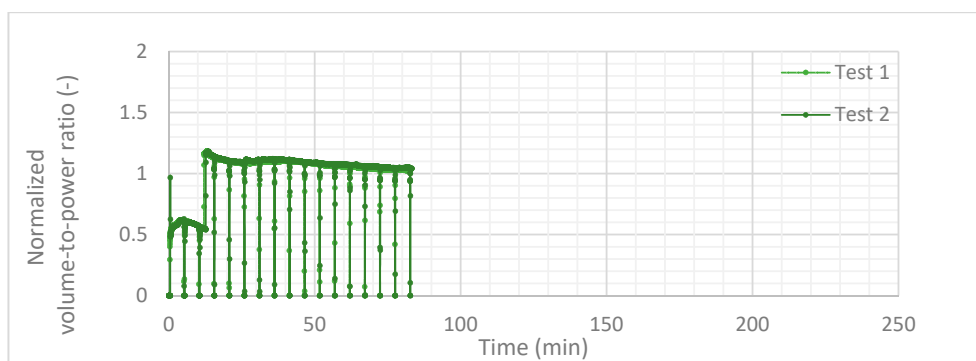


Figure A15. Normalized volume-to-power ratio at the thermostatic temperature of -20 °C.

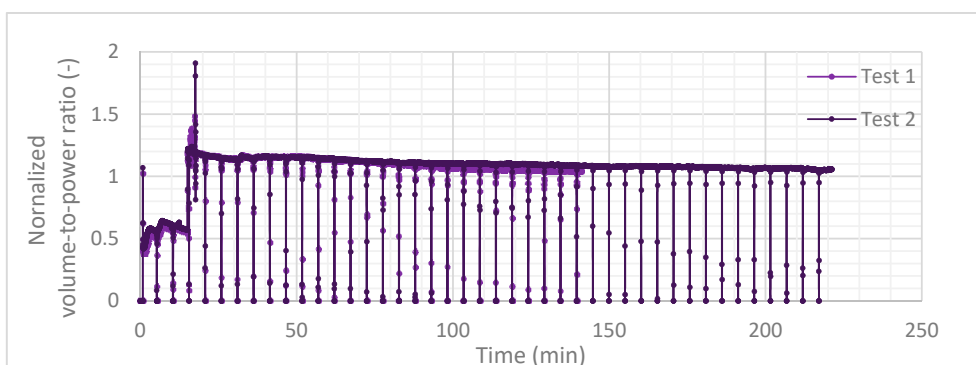


Figure A16. Normalized volume-to-power ratio at the thermostatic temperature of -30 °C.

References

1. Lopez, I.; Ibarra, E.; Matallana, A.; Andreu, J.; Kortabarria, I. Next generation electric drives for HEV/EV propulsion systems: Technology, trends and challenges. *Renew. Sustain. Energy Rev.* **2019**, *114*, 109336. [[CrossRef](#)]
2. Ghosh, A. Possibilities and Challenges for the Inclusion of the Electric Vehicle (EV) to Reduce the Carbon Footprint in the Transport Sector: A Review. *Energies* **2020**, *13*, 2602. [[CrossRef](#)]
3. Ertrac, E.; SNET, E. *ETIP SNET European Roadmap Electrification of Road Transport*, 3rd ed.; ERTRAC: Brussels, Belgium, 2017; pp. 8–14.
4. Seo, J.; Park, P.; Oh, Y.; Park, S. Estimation of Total Transport CO₂ Emissions Generated by Medium—and Heavy-Duty Vehicles (MHDVs) in a Sector of Korea. *Energies* **2016**, *9*, 638. [[CrossRef](#)]
5. *Electric Vehicle Outlook*; Bloomberg New Energy Finance: New York, NY, USA, 2020; Available online: <https://about.bnef.com/electric-vehicle-outlook/> (accessed on 20 April 2021).
6. Kulikov, I.; Kozlov, K.; Terenchenko, A.; Karpukhin, K. Comparative Study of Powertrain Hybridization for Heavy-Duty Vehicles Equipped with Diesel and Gas Engines. *Energies* **2020**, *13*, 1–23. [[CrossRef](#)]
7. Rupp, M.; Schulze, S.; Kuperjans, I. Comparative Life Cycle Analysis of Conventional and Hybrid Heavy-Duty Trucks. *World Electr. Veh. J.* **2018**, *9*, 33. [[CrossRef](#)]
8. *Global EV Outlook*; International Energy Agency: Paris, France, 2020; Available online: <https://www.iea.org/reports/global-ev-outlook-2020> (accessed on 20 April 2021).
9. Badin, F.; Le Berr, F.; Briki, H.; Dabadie, J.C.; Petit, M.; Magand, S.; Condemine, E. Evaluation of EV's energy consumption influencing factors: Driving conditions, auxiliaries use, driver's aggressiveness. *World Electr. Veh. J.* **2013**, *6*, 112–123. [[CrossRef](#)]
10. Pettersson, N.; Johansson, K.H. Modelling and control of auxiliary loads in heavy vehicles. *Int. J. Control* **2006**, *79*, 479–495. [[CrossRef](#)]
11. Winter, M.; Pretsch, S. Electrification of a commercial vehicle's auxiliaries: A change of reducing fuel consumption and CO₂ emissions. In Proceedings of the HVTT12: 12th International Symposium on Heavy Vehicle Transport Technology, Stockholm, Sweden, 16 September 2012.
12. Tretsiak, D.; Häberlein, T.; Bäker, B. Energy Efficient Control of the Air Compressor in a Serial Hybrid Bus based on Smart Data. *IFAC PapersOnLine* **2016**, *49*, 385–392. [[CrossRef](#)]
13. Wei, C.; Hofman, T.; Caarls, E.I.; van Iperen, R. A Review of the Integrated Design and Control of Electrified Vehicles. *Energies* **2020**, *13*, 1–31. [[CrossRef](#)]
14. Subramanian, S.C.; Darbha, S.; Rajagopal, K.R. A Diagnostic System for Air Brakes in Commercial Vehicles. *IEEE Trans. Intell. Transp. Syst.* **2006**, *7*, 360–375. [[CrossRef](#)]
15. van Gompel, P.; Koornneef, G. The Climatic-Altitude Chamber as Development and Validation Tool. SAE Technical Paper 2010-01-1294. 2010. Available online: <https://www.sae.org/publications/technical-papers/content/2010-01-1294/> (accessed on 18 June 2021). [[CrossRef](#)]
16. Li, H.; Jiang, W.; Sun, Z.; Zhu, Z. Experimental Investigation on Reciprocating Air Compressor Performance. *Advanced Materials Research* **2011**, *230–232*, 1269–1273. [[CrossRef](#)]
17. Valenti, G.; Murgia, S.; Costanzo, I.; Ravidà, A.; Piscopiello, G.P. Experimental investigation on the extreme cold start-up of an air compressor for electric heavy vehicles. *IOP Conf. Ser. Mater. Sci. Eng.* **2019**, *604*. [[CrossRef](#)]
18. Valenti, G.; Murgia, S.; Contaldi, A.; Valenti, A. Experimental evidence of the thermal effect of lubricating oil sprayed in sliding-vane air compressors. *Case Stud. Therm. Eng.* **2014**, *4*, 113–117. [[CrossRef](#)]
19. Contaldi, G. Rotary Compressor with Improved Working Efficiency and Relative Method. EP1798416B1, 2005.
20. Contaldi, G. Sistema Anticondensa per Compressore D'aria e Relativo Metodo. ITMI20060182A1, 2006.
21. Contaldi, G.; Murgia, S. Oil Separator for a Compressor and Compressor Assembly Comprising Said Separator. WO2018198037A1, 2017.
22. Contaldi, G.; Murgia, S. Vane Compressor with an Improved Lubrication System/Compressore a Palette Con Sistema di Lubrificazione Perfezionato. WO2019021252A1, 2019.